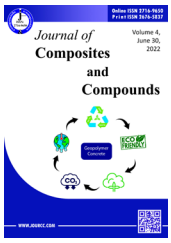

Available online at www.jourcc.com

Journal homepage: www.JOURCC.com

Journal of Composites and Compounds

Synthesis, feasibility study of production of singlet oxygen and hydroxyl radical and performance in antibacterial activity of ZnS:Eu QDs

Merat Karimi [a], Ehsan Sadeghi [b], Samira Khosravi Bigdeli [a], Mostafa Zahedifar [b]*

[a] Institute of Nanoscience and Nanotechnology, University of Kashan, Kashan, Iran
[b] Department of Physics, University of Kashan, Kashan, Iran

ABSTRACT

Eu doped zinc sulfide quantum dots (QDs) were prepared by the chemical Co-precipitation method. X-ray diffraction analysis (XRD), scanning electron microscopy (SEM) and infrared Fourier transform (FT-IR) analysis were used to characterize the quantum dots. The size of nano-crystals was estimated using a Williamson Hall equation. Then, the synthesized nanoparticles were studied to investigate the antibacterial effect, containing different strains of pathogenic bacteria, and the lowest inhibitory concentration and halo diameter were calculated. Williamson Hall equation of about 6 nm with a strain of 0.7 nm, which is match with the reported size of the SEM image. The photoluminescence spectrum (PL) of ZnS:Eu QD in excitation wavelength of 280 nm shows two emission peaks at 384 and 715 nm. In order to use these QDs as photosensitizer in photodynamic therapy, anthracene and methylene blue chemical detectors were used for detection of singlet oxygen and hydroxyl radical, respectively. The significant point for these quantum dots is that, in addition to production of hydroxyl radical, they also have the ability to produce singlet oxygen with UVC radiation. The antimicrobial effect of ZnS:Eu QDs was also investigated using a disc diffusion method on 11 microbial strains. The results of this test showed that Two microorganisms S.dysenteriae, Serotype that were resistant to the antibiotic nystatin and showed the highest sensitivity to ZnS:Eu QDs.

Peer review under responsibility of JCC Research Group

ARTICLE INFORMATION

Article history:
Received 2 March 2022
Received in revised form 21 April 2022
Accepted 20 June 2022

Keywords:
Nanoparticles
ZnS:Eu
Co-precipitation
Antibacterial
Cancer

1. Introduction

Due to the different applications of nanoparticles, different synthesis methods have been developed and used for these materials. The method used in the synthesis of nanoparticles is very important because it determines the size, shape and stability of the prepared particles. Also, the presence of a fine-grained microstructure with a high specific surface area can improve its properties. There are different methods for making nanoparticles. It should be noted that raw materials will have a significant effect on the functional properties of the material, which has many applications. They can be used in biological materials, antimicrobial applications, in the treatment of cancer, and to study its photocatalytic properties. And it has a great effect on environmental pollutants that can eliminate them. Many substances such as tin oxide, Dy_2O_3-SiO_2, $CoFe_2O_4$@SiO_2@$Dy_2Ce_2O_7$, $BiVO_4$, PrVO4/CdO, NiO, Zn – Co – O have the greatest effect on environmental pollutants and cause its purification [1-8]. Nanoparticles can also be used to target drugs. Chemical nanoparticles can be toxic, so use natural substances to target drugs, such as nano-gelatin, which has minimal side effects [9].

Photodynamic therapy (PDT) is a relatively new method for treating cancer in which tumor cells are destroyed by reactive oxygen species (ROS), such as singlet oxygen [10-12]. ROS are produced by photosensitizer that should be placed close to the tumor cells and is usually prescribed systematically. The advent of nanostructures provided new possibilities for PDT [13-15]; which of these, nanoparticles were used as a photosensitizer, photosensitizer drug carriers and so on. Although several types of nanoparticles have been used as potential candidates for PDT detection, but semiconductor nanocrystals (quantum dots) clearly produce singlet oxygen [16-18]. The luminescence properties of ZnS nanoparticles are changed by adding impurities to transition metals and rare earth metals (RE) that are optically and magnetically active [19-22]. ZnS is one of the materials compatible with the environment and it has a relatively large energy gap of about 3.68 eV at room temperature with a large binding *energy* [23]. Bacterial infections are one of the leading causes of many diseases and may lead to death and drug resistance to bacteria has caused increasing concern [24]. Recently, nanoparticles are widely used in antimicrobial activity because their ratio of surface to volume has increased as the size of particles decreases, so the antioxidant activity of nanoparticles increases and they have a huge impact on bacteria by removing it [16, 25, 26]. In order to improve the properties of the material and to have the most effective nanoparticles against radiation, it is to improve the original material by doping impurities in the main lattice and changing the energy levels of these nanoparticles improved in catalytic and fabrication processes Solar Cell and nanod-

* *Corresponding author: Ehsan Sadeghi; E-mail: sdgh@kashanu.ac.ir*
https://doi.org/10.52547/jcc.4.2.2

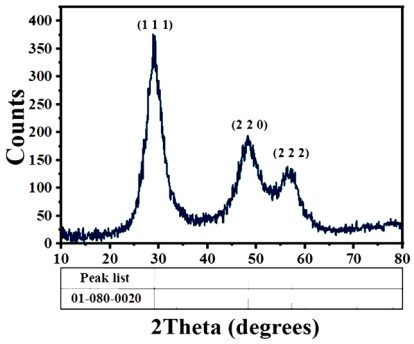

Fig. 1. X-ray diffraction patterns of the synthesized ZnS:Eu QDs.

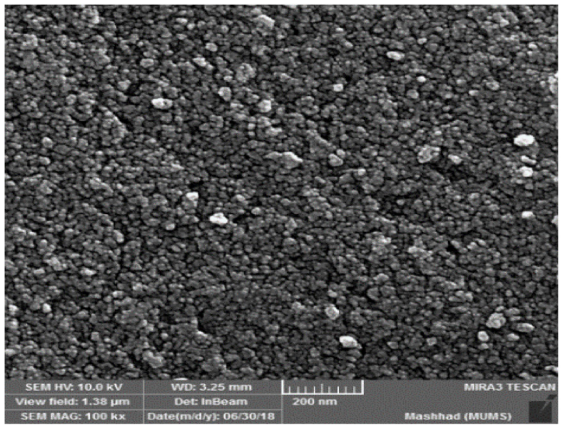

Fig. 3. SEM image of prepared ZnO:Eu QDs.

rugs [4, 5, 8].

The mechanism of mineral metal nanoparticles against pathogenic microbes is significant for a achieving synergistic effects with natural compounds. In a wide range of applications, the hypothetical mechanism of cytotoxicity shown by metal nanoparticles occurs through the release of ROS-reactive oxygen species. Ions lead to the production of reactive oxygen species in which oxygen radicals react with the membrane and cell components of the bacterial cell and other cellular components (such as mitochondria), causing their irreversible changes and causing the death of the bacterial cell [27-29]. Recently, group II-IV semiconductor nanoparticles have been used in medical and antibacterial fields due to their biocompatibility and unique properties. ZnS is biocompatible and semiconductor material which has a direct and extensive bandwidth of 3.61 eV and is used to fight bacteria [30-32]. Zinc sulfide is capable of producing red, blue and green luminescence due to the depletion of RE.

In this research, zinc sulfide QDs were produced with europium impurity and structural properties and its emission were investigated. The ability of these nanoparticles to produce singlet oxygen and hydroxyl radical was investigated using reagents of anthracene and methylene blue, respectively. The effects of ZnS:Eu QDs on 11 microorganisms were also investigated.

2. Materials and methods

ZnS:Eu QDs were synthesized using a Co-precipitation chemical methods. In this regard, zinc acetate [$(CH_3COO)_2Zn.2H_2O$], Brij-35, Europium(III) nitrate (Eu $(NO_3)_3$), and Sodium sulfide [Na_2S] were purchased from Merck, and used without further purification.

1.075 g zinc acetate was mixed with 0.5 mol% of Europium(III) nitrate in deionized water, and the resultant solution was placed on a magnetic stirrer to homogenize it during 60 min at room temperature (25°C),

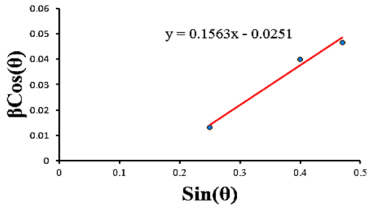

Fig. 2. Graph calculation strain and size ZnO:Eu QDs.

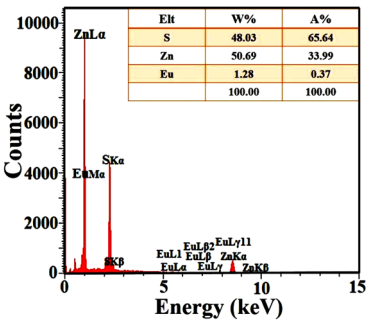

Fig. 4. EDS spectra of ZnS: Eu QDs. The percentage of elements in the attached table is shown in the figure.

Brij-35 with a volume ratio of 1:1 was added to the solution of the mixture, and it was placed on a magnetic stirrer (1500 rpm) for 2 h at 25°C. Sodium sulfide dissolved in deionized water was added to the solution, which was obtained in this step a milky and completely smooth solution. All steps were carried out at room temperature and also, to remove the extra salts in the precipitate prepared, several times the washing step was repeated with ionization water using centrifuges, then the resulting precipitate was placed in an oven for 2 h at 90 °C. In this step, the quantum dots of europium doped zinc sulfide were obtained.

For structural analysis and check fuzzy conditions, patterns of X-ray diffraction (XRD) using CuKα radiography X-rays nickel filtered were recorded. The scanning electron microscope (SEM) of the MIRA3 FEG-SEM-TESCAN model was used to study the microstructures of the quantum dots and the functional groups in the structure were characterized by spectrum from the Fourier transform infrared spectrometer (FT-IR) of the MagnaIR550 model. Optical properties of quantum dots using photoluminescence spectroscopy of Perkinelmer LS55 model and xenon arc as an excitation source at room temperature and also UV-Vis spectroscopy were evaluated to UV-Vis spectrometer (UVS-2500, PHYSTEC, Iran).

3. Results and discussion

3.1. XRD, SEM and energy dispersive spectrometry (EDS) analysis

As shown in Fig. 1, the XRD pattern confirms the structure of europium doped zinc sulfide quantum dots. The main peaks of ZnS:Eu related to the crystalline plates (1 1 1), (2 2 0) and (1 1 3) that these peaks correspond to the reference spectrum of 80-0020, which indicates the crystalline structure of ZnS:Eu is cubic.

Crystal structure was investigated using X-ray diffraction (XRD; model: Philips X'pert Pro MPP with Cu Kα radiation filtered by Ni, and λ= 0.1540 nm) analysis. In this regard, the average crystallite size (*D*) of ZnS:Eu NPs was estimated based on the Scherrer formula as given below:

$$D = \frac{K\lambda}{\beta \cos\theta} \quad (1)$$

[33]. Moreover, the average crystallite size is obtained to be about 6 nm. One of the defects that can express in Sheerer's method is that the peak broadening is only related to the crystallite size. While stud-

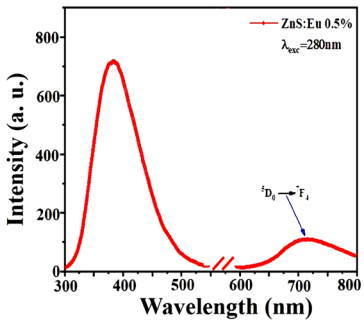

Fig. 5. Emission PL spectra of the synthesized ZnS:Eu QDs in excitation wavelength of 280 nm.

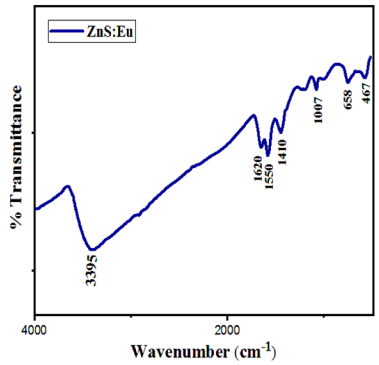

Fig. 7. FT-IR spectra of ZnS:Eu QDs.

ies show that the width the peak is in addition to the grain size to the strained lattice depended, so the Williamson-Hall equation can be used to solve the problem. According to this equation, the size of the grain and the strain lattice can be introduced as the factor of broadening the peak. So:

$$\beta = \beta_S + \beta_D \quad (2)$$

broadening of intensity peak due to grain size and peak broadening due to strain lattice broadening. The strain lattice broadening cause reduces or increases the distance between the crystalline plates. According to Bragg's law, by changing the distance between the crystalline plates, the angle where the peak is seen changes and this change leads to peak broadening. The Williamson Hall relationship is presented as follows [34]:

$$\beta\cos\theta = 2\varepsilon\sin\theta + \frac{0.9\lambda}{D} \quad (3)$$

By graph plotting the βCosθ versus Sinθ, is the slope representing the strain in the nanoparticles (Fig. 2). Also, by calculating the intercept, the grain size can be calculated; therefore, according to the calculations, the crystallite size about 6 nm with a strain 0.07 was measured.

The size of the QD obtained from the SEM image is also well coordinated with X-ray diffraction, which implies that the nanostructure is formed. The SEM image is shown in Fig. 3, which is a good homogeneity. On the other hand, Fig. 4 shows the EDS spectrum of the ZnS:Eu. The presence of the elements Zn, S and Eu with respective atomic percentages of 33.99%, 65.65%, and 0.5% is confirmed with the stoichiometric amount.

3.2. PL and FTIR analysis

The photoluminescence spectrum in excitation wavelength of 280 nm of europium doped zinc sulfide QDs is shown in Fg. 5. Usually, emission bands in the visible and ultraviolet region in the photoluminescence spectrum ZnS:Eu QDs can be seen. In this spectrum, two peaks are observed in wavelengths of 384 and 715 nm. Emission peak at 384 nm of zinc sulfide QDs is due to lattice defect. Also, the emission peak

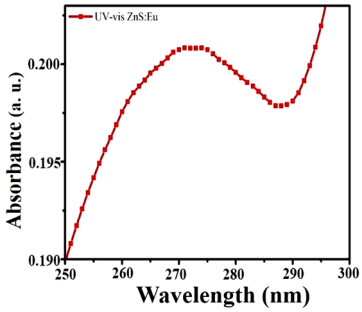

Fig. 6. UV-Vis absorption spectra of ZnS:Eu QDs.

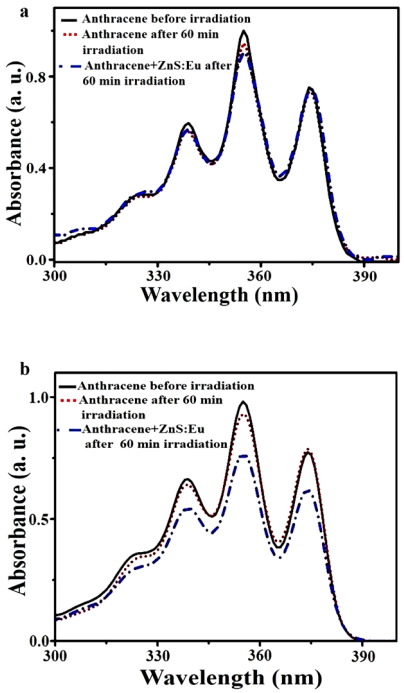

Fig. 8. UV-Vis spectra of anthracene and anthracene+ZnS:Eu before and after irradiation with a) UV-A and b) UV-C sources.

at 715 nm is related to the Eu^{3+} ion due to the transition of $^5D_0$ to $^7F_4$ [35-39]. Fig. 6 shows the visible-ultraviolet absorption spectrum of europium doped zinc sulfide quantum dots that a absorption peak at 272 nm is seen.

The FTIR absorption spectra of europium doped zinc sulfide QDs is shown in Fig. 7. The absorption peaks in the region 1359-1450 is related to the stretching vibrations of the C-O and the absorption spectrum in the 1620 is correspond to stretching group of the S-O [40]. The absorption peaks at the 467 , 658 and 1007 regions are related to the stretching vibrations of the Zn-S [41]. In the 3395 region, an absorption peak is observed, which corresponds to the O-H bond.

3.3. Singlet oxygen and hydroxyl radical production

The structure of anthracene changes in the presence of singlet oxygen and is converted to anthraquinone and therefore the absorption or emission of anthracene reduced. To access a correct evaluation of the value singlet oxygen, six samples from anthracene solution and anthracene solution along with europium doped zinc sulfide QDs at the same concentrations were made and the absorption spectra before and after irradiation with light sources of UV-A and UV-C was recorded. In Fig. 8a,b, the anthracene absorption spectra are observed in irradiation of different UV wavelengths. The decrease in the absorption intensity of anthracene after irradiation demonstrates the production of singlet oxygen and the greater reduction indicate the more production of singlet oxygen. As for the spectrum shown in Fig. 8a that is case irradiated located with

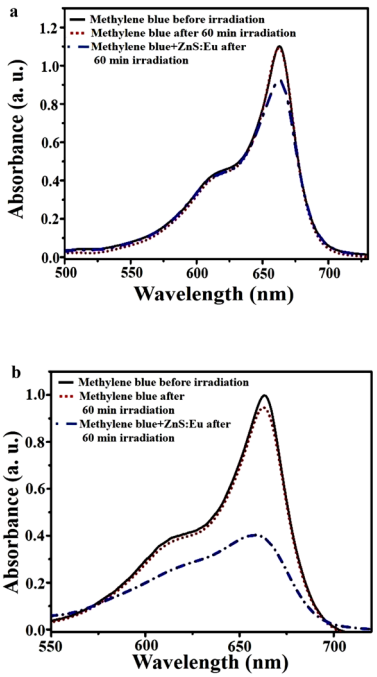

Fig. 9. UV-Vis spectra of methylene blue and methylene blue+ZnS:Eu before and after irradiation with a) UV-A and b) UV-C sources.

the UV-A source, can't be seen much reduction in absorption intensity of the anthracene solution or anthracene+ZnS:Eu QDs solutions, indicating that in this area of wavelengths is not produced the singlet oxygen. With observing the spectra located in Fig. 8b, the decrease in the absorption intensity of anthracene+ZnS:Eu QDs solutions after UV-C irradiation is signally seen while such a decrease is not yet observed for the anthracene sample alone, which can be attributed to the production of singlet oxygen at the presence of europium doped zinc sulfide QDs in the anthracene solution.

The MB is a dye type that oxidized in the presence of hydroxyl radical and decomposes into CO_2 and H_2O. According to the Beer–ambert law, the MB concentration affects the methylene blue absorbance, so the destruction of methylene blue structure leads to a decrease in its absorption intensity [1, 42, 43]. Hydroxyl radical was detected using methylene blue as a free radical sensor. For this purpose, as mentioned in the section of singlet oxygen detection, six samples with the same concentrations with and without the presence of synthesized QDs in methylene blue solution were prepared and were exposed at different wavelengths of UV. In Fig. 9a that is related to irradiation source of UV-A, reducing of the intensity of methylene blue absorption is not observed for any of samples of methylene blue-alone and methylene blue+ synthesized QDs, but on the spectra shown in Fig. 9a,b, a significant decrease of the absorption intensity is seen after UV-C irradiation, that indicating the production of hydroxyl radicals in the presence of europium doped zinc sulfide quantum dots.

3.4. Disk diffusion assay

The diffusion disc method was used to evaluate the susceptibility and resistance of bacteria against antibacterial. This method was performed according to CLSI (Clinical and laboratory standards institute). The test was performed on sheets Mueller Hinton Media contains Agar culture medium and wells with a diameter of 0.6 mm on the culture medium, then 100 µl of bacterial suspensions with turbidity equivalent to 0.5 McFarland at the same condition was cultivated. ZnS:Eu QDs were dissolved in dimethyl sulfoxide to a concentration of 30 mg/ml. The amount of 10 µl, equivalent to 300 µg, was poured into each sump of QDs inside the sumps, the plates were placed at incubator in a temperature of 37 °C for 24 h and its antimicrobial activity was obtained for each microorganism to measuring the growth aura. In the larger diameter of the aura, the bacterium is more sensitive to the antibacterial. In this study, ZnS:Eu QDs were introduced as an antibacterial substance. This test is used to evaluate the antimicrobial activity of nanoparticles using 11 microorganisms shown in Table 1. In the diffusion disc, the diameter

Table 1.
The results of the evaluate the antimicrobial activity of ZnS;Eu QDs using 11 microorganisms.

Test microorganisms	ZnS: Eu		Antibiotics					
			Rifampin		Gentamicin		Nystatin	
	DD[a]	MIC[b]	DD[a]	MIC[b]	DD[a]	MIC[b]	DD[a]	MIC[b]
B.subtilis	9	125	19	31.25	22	3.90	NA	NA
S.epidermidis	-	62.50	27	1.95	45	1.95	NA	NA
S.aureus	-	125	11	1.95	20	1.95	NA	NA
E.coli	-	62.50	11	3.90	20	3.90	NA	NA
K.pneumonia	-	62.50	8	15.63	17	3.90	NA	NA
S.dysenteriae	-	31.25	9	15.36	17	3.90	NA	NA
S.paratyphi-A serotype	-	31.50	8	15.63	18	3.90	NA	NA
P.aeruginosa	-	62.50	-	31.25	20	7.81	NA	NA
S.pyogenes	-	125	21	0.975	32	0.975	NA	NA
A.niger	-	-	NA	NA	NA	NA	27	31.2
C.albicans	-	62.50	NA	NA	NA	NA	27	31.2

A dash (–) indicate no antimicrobial activity.

[a] DD (Disk diffusion method), Inhibition zones in diameter (mm) around the impregnated disks.

[b] MIC (Minimal Inhibition concentrations as µg/ml), NA (Not applicable).

of the measured growth retardation aura showed sensitivity only to the bacterium B.subtilis, and the installation drop was 9 mm and it didn't have any great effect on other bacteria.

3.5. Minimum inhibitory concentration

In order to determine the better performance and effectiveness of the synthesized QDs on microorganisms, the analysis of determining the minimum inhibitory concentration (MIC) was studied. MIC is the lowest inhibitory concentration that prevents microbes from growing. This analysis was calculated for susceptible microorganisms by micro-well dilution assay. For this purpose, micro-pages of 96 sterile houses were prepared. For each of the plates, 95 µl of culture medium, 5 µl of bacterial suspension were diluted with 0.5 ml of McFarland and 100 µl of the QDs were added and then the plate was heated in an incubator at 37 °C for 24 h. MIC was also calculated for nanoparticles and the obtained results were reported in Table 1. Eleven microbial strains showed a great sensitivity to low yields under experiment. By increasing the concentration of nanoparticles, the inhibitory effect of microorganisms is increased. The highest susceptibility of ZnS:Eu nanoparticles to C.Albicans microorganisms, which are classified as fungi, was determined. Nanoparticles had a relatively good inhibitory effect on other bacteria.

4. Conclusion

Synthesis of europium doped zinc sulfide QDs was done to Co-precipitation method. Using XRD, SEM and EDS analysis the structural properties of the synthesized nanoparticles were studied. In the ZnS:Eu photoluminescence spectra, two peaks are observed that the peak related to in the ultraviolet region and the visible region due to lattice defects and Eu^{3+} ion, respectively. In order to investigation of the applicability of ZnS:Eu QDs in the treatment of photodynamic therapy, two chemical reagents of anthracene and methylene blue were used for detection of singlet oxygen and hydroxyl radical, respectively. According to obtained results of absorption spectrum of anthracene and methylene blue solutions, In the presence of quantum dots, production of singlet oxygen and hydroxyl radical was proved. These results shows that only under irradiation of UV-C, the hydroxyl radicals and singlet oxygen are produced and the UV-A light is not proper source for excitation of the synthesized QDs. Also ZnS:Eu nanoparticles showed inhibitory effects against microorganisms. The largest diameter of the non-growth aura is assigned to the bacterium B.subtilis and the minimum inhibitory concentration of nanoparticle growth is assigned to the gram-negative bacterium C.Albicans.

Acknowledgements

The authors want to express their thanks from the University of Kashan for the supports in conducting this research.

REFERENCES

[1] S. Zinatloo-Ajabshir, M. Mousavi-Kamazani, Recent advances in nanostructured Sn−Ln mixed-metal oxides as sunlight-activated nanophotocatalyst for high-efficient removal of environmental pollutants, Ceramics International 47(17) (2021) 23702-23724.

[2] K. Mahdavi, S. Zinatloo-Ajabshir, Q.A. Yousif, M. Salavati-Niasari, Enhanced photocatalytic degradation of toxic contaminants using Dy_2O_3-SiO_2 ceramic nanostructured materials fabricated by a new, simple and rapid sonochemical approach, Ultrasonics Sonochemistry 82 (2022) 105892.

[3] S. Zinatloo-Ajabshir, S.A. Heidari-Asil, M. Salavati-Niasari, Rapid and green combustion synthesis of nanocomposites based on Zn–Co–O nanostructures as photocatalysts for enhanced degradation of acid brown 14 contaminant under sunlight, Separation and Purification Technology 280 (2022) 119841.

[4] M. Mousavi-Kamazani, Facile hydrothermal synthesis of egg-like BiVO4 nanostructures for photocatalytic desulfurization of thiophene under visible light irradiation, Journal of Materials Science: Materials in Electronics 30(19) (2019) 17735-17740.

[5] M. Mousavi-Kamazani, M. Ghodrati, R. Rahmatolahzadeh, Fabrication of Z-scheme flower-like AgI/Bi2O3 heterojunctions with enhanced visible light photocatalytic desulfurization under mild conditions, Journal of Materials Science: Materials in Electronics 31(7) (2020) 5622-5634.

[6] S. Zinatloo-Ajabshir, M. Salavati-Niasari, Preparation of magnetically retrievable $CoFe_2O_4$@SiO_2@$Dy_2Ce_2O_7$ nanocomposites as novel photocatalyst for highly efficient degradation of organic contaminants, Composites Part B: Engineering 174 (2019) 106930.

[7] F. Motahari, M.R. Mozdianfard, M. Salavati-Niasari, Synthesis and adsorption studies of NiO nanoparticles in the presence of H_2 acacen ligand, for removing Rhodamine B in wastewater treatment, Process Safety and Environmental Protection 93 (2015) 282-292.

[8] R. Monsef, F. Soofivand, H. Abbas Alshamsi, A. Al-Nayili, M. Ghiyasiyan-Arani, M. Salavati-Niasari, Sonochemical synthesis and characterization of $PrVO_4$/CdO nanocomposite and their application as photocatalysts for removal of organic dyes in water, Journal of Molecular Liquids 336 (2021) 116339.

[9] A.S. Zinatloo, Q.N. Taheri, Effect of some synthetic parameters on size and polydispersity index of gelatin nanoparticles cross-linked by CDI/NHS system, (2015).

[10] S.B. Brown, E.A. Brown, I. Walker, The present and future role of photodynamic therapy in cancer treatment, The lancet oncology 5(8) (2004) 497-508.

[11] M. Zahedifar, E. Sadeghi, M. Shanei, A. Sazgarnia, M. Mehrabi, Afterglow properties of CaF2: Tm nanoparticles and its potential application in photodynamic therapy, Journal of Luminescence 171 (2016) 254-258.

[12] D. Lee, S. Kwon, S.-y. Jang, E. Park, Y. Lee, H. Koo, Overcoming the obstacles of current photodynamic therapy in tumors using nanoparticles, Bioactive Materials (2021).

[13] C. Liu, Research and development of nanopharmaceuticals in China, science 1 (1990) 15.

[14] Y. Zhang, Relationship between Size and Function of Natural Substance Particles, Nano Biomedicine & Engineering 3(1) (2011).

[15] F. Tavakkoli, M. Zahedifar, E. Sadeghi, Effect of LaF3: Ag fluorescent nanoparticles on photodynamic efficiency and cytotoxicity of Protoporphyrin IX photosensitizer, Photodiagnosis and photodynamic therapy 21 (2018) 306-311.

[16] X. Nie, C. Jiang, S. Wu, W. Chen, P. Lv, Q. Wang, J. Liu, C. Narh, X. Cao, R.A. Ghiladi, Carbon quantum dots: A bright future as photosensitizers for in vitro antibacterial photodynamic inactivation, Journal of Photochemistry and Photobiology B: Biology 206 (2020) 111864.

[17] M. Roeinfard, M. Zahedifar, M. Darroudi, A.K. Zak, E. Sadeghi, Synthesis of Graphene Quantum Dots Decorated With Se, Eu and Ag As Photosensitizer and Study of Their Potential to Use in Photodynamic Therapy, Journal of Fluorescence 31(2) (2021) 551-557.

[18] W.M.O. de Santana, B.L. Caetano, S.R. de Annunzio, S.H. Pulcinelli, C. Ménager, C.R. Fontana, C.V. Santilli, Conjugation of superparamagnetic iron oxide nanoparticles and curcumin photosensitizer to assist in photodynamic therapy, Colloids and Surfaces B: Biointerfaces 196 (2020) 111297.

[19] H. Hu, W. Zhang, Synthesis and properties of transition metals and rare-earth metals doped ZnS nanoparticles, Optical materials 28(5) (2006) 536-550.

[20] M.R. Kim, J.H. Chung, D.-J. Jang, Spectroscopy and dynamics of Mn^{2+} in ZnS nanoparticles, Physical Chemistry Chemical Physics 11(6) (2009) 1003-1006.

[21] G. Yue, P. Yan, D. Yan, X. Fan, M. Wang, D. Qu, J. Liu, Hydrothermal synthesis of single-crystal ZnS nanowires, Applied Physics A 84(4) (2006) 409-412.

[22] E. Sadeghi, Z. Mahmoodian, M. Zahedifar, Synthesis of Nanoparticles of ZnS: Ag-L-cysteine-protoporphyrin IX Conjugates and Investigation its Potential of Reactive Oxygen Species Production, Journal of fluorescence 29(5) (2019) 1089-1101.

[23] Z.H. Ibupoto, K. Khun, X. Liu, M. Willander, Hydrothermal synthesis of nanoclusters of ZnS comprised on nanowires, Nanomaterials 3(3) (2013) 564-571.

[24] E.B. Hirsch, V.H. Tam, Detection and treatment options for Klebsiella pneumoniae carbapenemases (KPCs): an emerging cause of multidrug-resistant infection, Journal of antimicrobial chemotherapy 65(6) (2010) 1119-1125.

[25] P.K. Singh, P.K. Sharma, M. Kumar, R. Dutta, S. Sundaram, A.C. Pandey, Retracted Article: Red luminescent manganese-doped zinc sulphide nanocrystals and their antibacterial study, Journal of Materials Chemistry B 2(5) (2014) 522-528.

[26] R. Kumar, P. Sakthivel, P. Mani, Structural, optical, electrochemical, and antibacterial features of ZnS nanoparticles: incorporation of Sn, Applied Physics A 125(8) (2019) 543.

[27] X. Duan, X. Huang, X. Wang, S. Yan, S. Guo, A.E. Abdalla, C. Huang, J. Xie, l-Serine potentiates fluoroquinolone activity against Escherichia coli by enhancing endogenous reactive oxygen species production, Journal of Antimicrobial Chemo-

therapy 71(8) (2016) 2192-2199.
[28] M. Amiri, M. Salavati-Niasari, A. Pardakhty, M. Ahmadi, A. Akbari, Caffeine: A novel green precursor for synthesis of magnetic $CoFe_2O_4$ nanoparticles and pH-sensitive magnetic alginate beads for drug delivery, Materials Science and Engineering: C 76 (2017) 1085-1093.
[29] M. Karimi, M.A. Kashi, A.H. Montazer, Synthesis and characterization of ultrafine γ-Al_2O_3: Cr nanoparticles and their performance in antibacterial activity, Journal of Sol-Gel Science and Technology 99(1) (2021) 178-187.
[30] R.Y. Pelgrift, A.J. Friedman, Nanotechnology as a therapeutic tool to combat microbial resistance, Advanced drug delivery reviews 65(13-14) (2013) 1803-1815.
[31] D. Diaz-Diestra, B. Thapa, J. Beltran-Huarac, B.R. Weiner, G. Morell, L-cysteine capped ZnS: Mn quantum dots for room-temperature detection of dopamine with high sensitivity and selectivity, Biosensors and Bioelectronics 87 (2017) 693-700.
[32] X. Wang, H. Huang, B. Liang, Z. Liu, D. Chen, G. Shen, ZnS nanostructures: synthesis, properties, and applications, Critical reviews in solid state and materials sciences 38(1) (2013) 57-90.
[33] B. Cullity, Elements of X-ray Diffraction. Addison and Wesley Publishing Company Inc, Reading, USA (1978) 32-106.
[34] G. Williamson, W. Hall, X-ray line broadening from filed aluminium and wolfram, Acta metallurgica 1(1) (1953) 22-31.
[35] Y. Wang, X. Liang, E. Liu, X. Hu, J. Fan, Incorporation of lanthanide (Eu^{3+}) ions in ZnS semiconductor quantum dots with a trapped-dopant model and their photoluminescence spectroscopy study, Nanotechnology 26(37) (2015) 375601.
[36] I. Ahemen, O. Meludu, F. Dejene, B. Viana, Site spectroscopy of Eu3+ doped-ZnS nanocrystals embedded in sodium carboxymethyl cellulose matrix, Optical Materials 61 (2016) 82-91.
[37] G.S. Lotey, Z. Jindal, V. Singhi, N. Verma, Structural and photoluminescence properties of Eu-doped ZnS nanoparticles, Materials Science in Semiconductor Processing 16(6) (2013) 2044-2050.
[38] M. Pal, N. Mathews, E.R. Morales, J.G. y Jiménez, X. Mathew, Synthesis of Eu+ 3 doped ZnS nanoparticles by a wet chemical route and its characterization, Optical Materials 35(12) (2013) 2664-2669.
[39] U.T.D. Thuy, A. Maurice, N.Q. Liem, P. Reiss, Europium doped In (Zn) P/ZnS colloidal quantum dots, Dalton transactions 42(35) (2013) 12606-12610.
[40] I.M. Ali, I.M. Ibrahim, E.F. Ahmed, Q.A. Abbas, Structural and Characteristics of Manganese Doped Zinc Sulfide Nanoparticles and Its Antibacterial Effect against Gram-Positive and Gram-Negative Bacteria, Open Journal of Biophysics 6(01) (2016) 1.
[41] L.-N. Liu, J.-G. Dai, T.-J. Zhao, S.-Y. Guo, D.-S. Hou, P. Zhang, J. Shang, S. Wang, S. Han, A novel Zn (ii) dithiocarbamate/ZnS nanocomposite for highly efficient Cr^{6+} removal from aqueous solutions, RSC advances 7(56) (2017) 35075-35085.
[42] Y. Abdollahi, A.H. Abdullah, Z. Zainal, N.A. Yusof, Photocatalytic degradation of p-Cresol by zinc oxide under UV irradiation, International journal of molecular sciences 13(1) (2012) 302-315.
[43] A.A. Mansur, H.S. Mansur, F.P. Ramanery, L.C. Oliveira, P.P. Souza, "Green" colloidal ZnS quantum dots/chitosan nano-photocatalysts for advanced oxidation processes: study of the photodegradation of organic dye pollutants, Applied Catalysis B: Environmental 158 (2014) 269-279.